# ISFA2022-040

# MODEL BASED REPETITIVE CONTROL FOR PEELING FRONT GEOMETRY CONTROL IN A ROLL-TO-ROLL PEELING PROCESS

Qishen Zhao<sup>1</sup>, Christopher Martin, Dongmei Chen, Wei Li Department of Mechanical Engineering, University of Texas at Austin Austin, TX, United States

## **ABSTRACT**

Roll-to-roll(R2R) peeling is an innovative method that transfers flexible electronics and 2D materials from the flexible substrate where they are grown to the end-use substrate. This process enables the full potential of R2R 2D material fabrication methods in a continuous, high-throughput, and environmentfriendly manner. During the R2R peeling process, the device patterning causes periodic changes in the adhesion energy between the device and substrate. This periodic disturbance can degrade the quality of the final product if not properly controlled. Current control methods used for the R2R peeling process do not explicitly reject the periodic disturbance. It is therefore desirable to develop a controller that is capable of performing periodic disturbance rejection. This paper presents a model-based repetitive controller that integrates a frequency estimation of the disturbance into the R2R peeling control to maintain the optimal peeling process performance. A linear estimator using system identification techniques is employed. The simulation results show that the developed controller achieves better R2R process performance when compared to a conventional model-based controller.

Keywords: Roll-to-roll peeling process, periodic disturbance, repetitive control

### 1. INTRODUCTION

For flat, flexible materials, roll-to-roll (R2R) production methods are desirable because they are continuous and are both more efficient and have higher throughput than discrete batch methods. For over a century R2R methods have been used to produce flexible products such as newspapers, diapers, and textiles. Recently, there has been significant research effort focused on applying R2R production concepts to the production

of flexible electronic devices and materials. Specifically, several R2R methods of growing 2D materials such as graphene have been developed [1, 2], and similar R2R methods have been developed for fabricating flexible electronics [3].

For flexible electronics, conventional transfer printing methods involve using discontinuous stamps to move the device from its growth substrate to a useful substrate [3, 4]. Similarly, conventional transfer methods for chemical vapor deposition (CVD) graphene are discrete batch methods, and they involve using toxic chemical etchants to dissolve the copper growth substrate before the graphene can be deposited onto a target substrate [2]. Thus, to take full advantage of the aforementioned continuous, high-throughput R2R production processes of 2D electronic devices, there is a need for a fully R2R dry transfer method that is environmentally benign. In [2], such an R2R transfer method is developed for CVD graphene, where few layer graphene was grown on a Ni foil and then mechanically peeled from that foil onto a polymer sheet in an R2R manner. To scale up the dry transfer process for commercialization, more research needs to be conducted. In [5], a critical peeling velocity is determined, below which the graphene will adhere to the growth substrate and above which it will adhere to a polymer target substrate. In [6], it was found that for certain 2D materials there is a peeling angle that optimizes the transfer quality. In [7], our group presents the results of an investigation of the effects of peeling velocity, roller diameter, and peeling angle on the transfer quality of CVD graphene using a prototype of the R2R dry transfer system, as illustrated in Fig. 2.1(a). We find that both peeling velocity and roller diameter are critical parameters.

In addition, in the realm of flexible electronics, flexible stamps have been developed with adhesion energies that vary based on peeling velocity and retraction angle, allowing them to

<sup>&</sup>lt;sup>1</sup> Contact author: qishenzhao0904@utexas.edu

pick up an electronic device from its growth substrate and then deposit the device onto a target substrate [5, 8, 9]. These stamps are flexible and their adhesion energy can be controlled through mechanical processes. Therefore, they could be integrated into a system with rollers to form a R2R process. Whether the transfer process is moving flexible electronics or 2D materials, the key dynamics for the R2R peeling process occur at the peeling front. An optimal control of the peeling front will ensure the required quality of the final product.

The peeling angles determine the geometry of the peeling front and thus the peeling front dynamics. However, it is difficult to control the peeling angles due to the highly nonlinear nature of the web peeling dynamics. Various control methods have been explored by our group including using a supervisory controller to control the peeling angles through the web tensions [7, 10] and building a robust full-state feedback controller using LMI constraints [11]. Despite successfully achieving the desired R2R process performance, these methods do not take full advantage of available a-priori knowledge of the disturbance frequencies to specifically target and minimize the dominant periodic disturbances acting on the R2R system. Non-ideal rollers and internal friction within the motors cause disturbances that have the same frequency as the roller speed [12], and many of the devices that the process transfers will have pre-defined patterns, meaning that there will be other predictable periodic disturbances related to the variation in the adhesion energy at the peeling front. This paper introduces a model-based controller specifically designed to reject periodic disturbances. A repetitive controller [13] for R2R peeling process is proposed in this paper to take advantage to the prior knowledge of the disturbance frequencies and use that information to augment a discretized linear model of the peeling system [10]. Using this augmented model, an optimal controller is presented that systematically rejects the periodic disturbances, allowing the peeling angles to remain near the desired value.

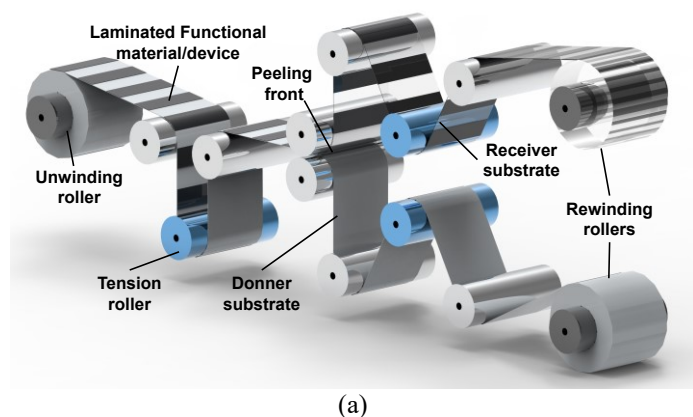
The structure of the paper is as follows. Section 2 presents an overview of the important system characteristics and parameters of the R2R dry transfer process. Section 3 describes how system identification methods are used to develop a discrete, linear, control-oriented model of the system. Section 4 describes the design process for the model-based repetitive controller. Section 5 compares the performance of the repetitive controller against that of a model-based controller that does not use a-priori disturbance frequency information. Finally, section 6 provides concluding remarks.

## 2. R2R DRY TRANSFER PROCESS

A typical R2R mechanical transfer printing process is shown in Fig. 1(a) [10]. The laminate of donor and receiver substrate is unwound from the unwinding roller. The patterns marked in black are initially attached on the donor substrate, which is rewound on the bottom rewinding roller. The mechanical peeling process transfers the patterns from the bottom substrate to the top substrate. The schematic of the process is shown in Fig. 1(b). The system has an unwinding speed  $v_1$ , controlled by a motor with rotational speed  $w_1$ , which is constant. The rewinding rollers have linear speeds of  $v_2$  and  $v_3$ . The rewinding rollers are actuated by the torques  $w_2$  and  $w_3$ . The webs on the three sides

of peeling front are subject to tensions  $t_1$ ,  $t_2$  and  $t_3$ . The peeling front geometry can be uniquely described with two peeling angles:  $\theta$  and  $\alpha$ , as shown in Fig. 1(c). The two angles define the loading condition of the peeling process. The peeling front geometry is dependent on the tensions of each side. The dynamics of the tensions depend on the roller velocities and peeling front velocity.

In a R2R process, the rollers rotate continuously during operation. Static friction in the motor and roller shaft will appear as a cyclic disturbance load. Eccentricity in roller shape may also cause periodic disturbances to the web during the R2R process. In addition to these common disturbances, for a R2R peeling process, the adhesion energy variation also acts as a disturbance to the system. The periodic change in adhesion can be seen in continuous transfer printing processes where patterns to be transferred are arranged in an equally spaced fashion, as shown in Fig. 1(c). The change in adhesion energy may cause variations in the web tensions and peeling angles, which causes periodic disturbances in the system. It is necessary to design a controller to reject these disturbances.



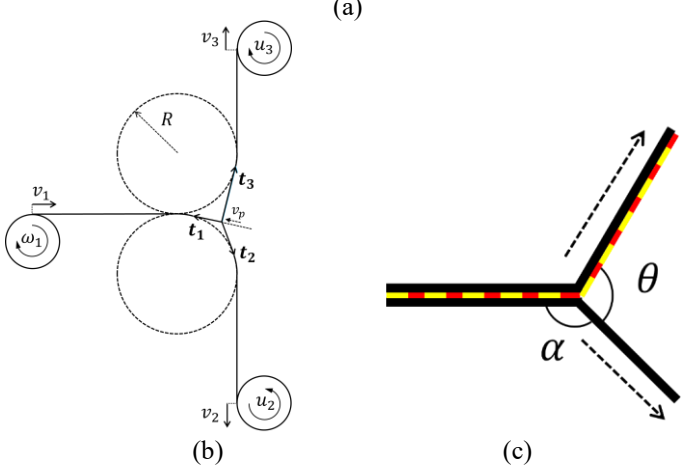


**FIGURE 1:** (a) R2R peeling system [10], (b) system schematic and (c) transferring of periodic patterns

### 3. SYSTEM MODEL FOR CONTROL DESIGN

Obtaining an accurate system model is a prerequisite for designing an effective controller. Since many system parameters, such as adhesion energy, web stiffness, friction coefficient, roller inertia etc., are unknown or varying with the system operation, it is highly challenging to develop a physics-based model. To overcome this hurdle, a system identification approach is introduced that utilizes the measurement data to obtain the state space system model.

## 3.1 System Identification Framework

The system to be controlled is nonlinear, but the control goal of the system in this study is to maintain the peeling angles at a constant level, so a linear model around the angle set point can be used as an approximation of the nonlinear system. A local linear system model identification framework based on a least-squares method is used here.

Based on the system model, the state of the system can be characterized by the tensions of the web  $t_1$ ,  $t_2$ ,  $t_3$  and the rotational speed of the rewinding rollers  $v_2$  and  $v_3$ . Assume that the system dynamics around an equilibrium peeling front geometry can be described as

$$x_{l}(k+1) = A_{l} \cdot x_{l}(k) + B_{l} \cdot u_{l}(k)$$
 (1)

where  $[t_1(k) \ t_2(k) \ t_3(k) \ v_2(k) \ v_3(k) \ \theta(k) \ \alpha(k)]^T$  is the state variable  $x_l(k)$  with the control objectives  $\theta(k)$  and  $\alpha(k)$  also included as states.  $u_l(k)$  is the control input vector that contains the motor torque control inputs  $[u_2(k) \ u_3(k)]^T$ .  $A_l$  is an unknown 7-by-7 matrix and  $B_l$  is an unknown 7-by-2 matrix. The tensions can be measured with load cells. The roller velocities can be measured with encoders. During the data collection process, system state measurements and control inputs are recorded. The series of measurements and input signals can be stacked as

$$X = \begin{bmatrix} | & | & | & | \\ x_{l}(1) & x_{l}(2) & \cdots & x_{l}(N-1) \end{bmatrix}$$

$$X' = \begin{bmatrix} | & | & | & | \\ x_{l}(2) & x_{l}(3) & \cdots & x_{l}(N) \\ | & | & | & | \end{bmatrix}$$

$$Y = \begin{bmatrix} | & | & | & | \\ u_{l}(1) & u_{l}(2) & \cdots & u_{l}(N-1) \\ | & | & | & | \end{bmatrix}$$
(2)

where N is the total number of measurements and X' is the one time-step shift matrix of X. By including the state measurements and control inputs, the following equation can be obtained from Eqs. (1) and (2):

$$X' = A_l \cdot X + B_l \cdot Y,\tag{3}$$

which can be rewritten as,

$$X' = \begin{bmatrix} A_l & B_l \end{bmatrix} \cdot \begin{bmatrix} X \\ \gamma \end{bmatrix}. \tag{4}$$

The state space matrices  $A_l$  and  $B_l$  can be obtained using

$$[A_l \quad B_l] = X' \cdot \begin{bmatrix} X \\ \gamma \end{bmatrix}^{\dagger} \tag{5}$$

where † is the Moore-Penrose pseudoinverse.

Since the goal of the system identification is to obtain a linear model around equilibrium peeling angles using the measurement data, the system should operate around the peeling angle configuration during the data collection process. The supervisory peeling angle control developed in our previous study [14] is utilized as a feedforward controller to allow the system to reach the vicinity of the peeling angle set point. A system identification process can then be conducted to obtain the linear system model to describe the system transient behavior around the equilibrium point.

The system identification framework of the R2R peeling system model around a particular peeling angle setpoint is shown in Fig. 2. The supervisory peeling angle controller maintains the peeling angle around the angle setpoint where a linear model is developed.

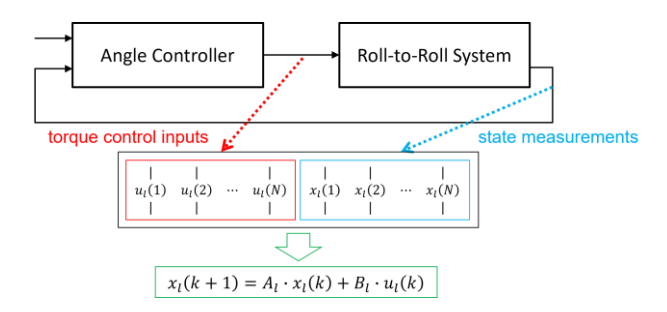


FIGURE 2: System identification process

#### 3.2 System Identification for Control Design

The system identification framework is verified using the nonlinear model developed in [10]. An example that represents a typical R2R peeling process is given bellow.

In this example, the objective is to obtain a linear system model around the peeling front configuration of  $\theta=90^\circ$  and  $\alpha=120^\circ$ . The adhesion energy is set as a constant of 150 N/m. The system is initially maintained at the equilibrium peeling condition. To introduce excitations to the system, the reference peeling angles are varied around the desired angles. The reference peeling angle signals into the peeling angle controller are set as uniform random variables around the desired peeling angle. Reference angle for  $\theta$  is a uniformly distributed variable between 85° and 95°, and the reference angle for  $\alpha$  varies between 115° and 125°. The reference angles profile is shown in Fig. 3. With the designed profile, the roller/tension and peeling angle dynamics along each direction can be captured in the response data. White noise is added to the data to represent the typical real-world measurements.

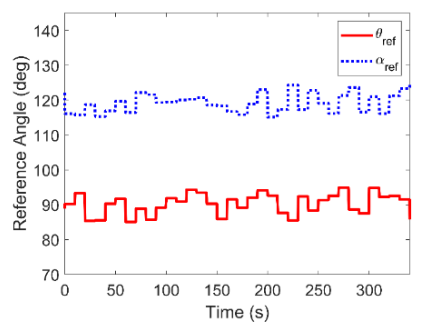


FIGURE 3: Reference angle for system identification

The estimated linear model is obtained through Eqn. (5) and is evaluated by comparing the model response with another set of input output data generated from the nonlinear system model. The comparison of the model response and measured response to the same torque input is shown in Fig. 4. The tension response comparison between model and data generated from nonlinear model is shown in Fig. 4(a). The velocity response is shown in Fig. 4(b). It is shown that the response of the simulation model captures the dynamics of the nonlinear system around the operating region. The tension and roller velocity dynamics are modeled fairly accurately.

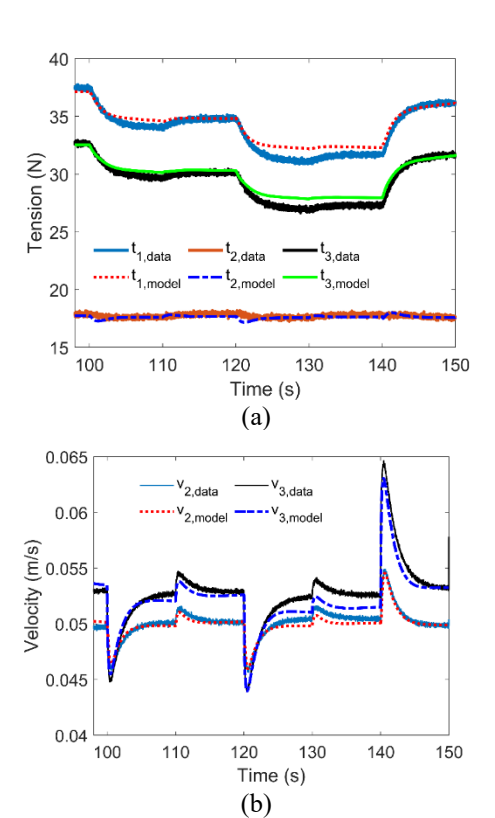


FIGURE 4: Model evaluation for (a) roller velocities, (b) tensions

## 4. CONTROL DESIGN

In this section, the design of the repetitive controller that rejects disturbances is presented. The linear model obtained in the previous section is used for the control design. The goal is to have the peeling angles regulated at the desired angle set point.

To reject the periodic disturbances, the model of the disturbances needs to be included in the control design. Since the spacing of patterns on the web is known in a R2R peeling process, and the speed of the R2R process can be directly measured, the period of the disturbance can be calculated. Assume the distance between two patterns is L. The period of the disturbance caused by the varying adhesion can be calculated as

$$\tau_1 = \frac{L}{v_n}.\tag{6}$$

The torque disturbances have the same frequency as that of the winding rollers. The periods of the disturbances can be expressed

$$\tau_i = \frac{2\pi R_i}{v_i}, i = 2,3 \tag{7}$$

The linear state-space model with disturbance included can be written in a discrete-time form as [13]:

$$x_l(k+1) = A_l \cdot x_l(k) + B_l \cdot u_l(k) + B_d \cdot \mu(k),$$
(8)

$$y_l(k) = C_l \cdot x_l(k) \tag{9}$$

where the system output are the two peeling angles  $[\theta(k) \ \alpha(k)]^T$  to be maintained.  $\mu(k)$  represents an unknown disturbance expressed as

$$\mu(k) = \frac{\varepsilon(k)}{D(z^{-1})} \tag{10}$$

where  $D(z^{-1})$  is the model of the disturbance. The disturbance model is modeled as

$$D(z^{-1}) = 1 - z^{-\gamma}. (11)$$

 $\gamma$  is the period of the disturbance. Here, since the disturbances considered in this study come from three sources with periods  $\tau_1$ ,  $\tau_2$  and  $\tau_3$ ,  $\gamma$  is the least common multiple of  $\tau_1$ ,  $\tau_2$  and  $\tau_3$ . Applying  $D(z^{-1})$  to the state equation gives

$$x_f(k+1) = A_I \cdot x_f(k) + B_I \cdot u_f(k) + B_d \cdot \varepsilon(k)$$
 (12)

where

$$x_f(k) = D(z^{-1})x_I(k) = x_I(k) - x_I(k - \gamma)$$
 (13)

$$u_f(k) = D(z^{-1})u_l(k) = u_l(k) - u_l(k - \gamma)$$
 (14)

and applying  $D(z^{-1})$  to the output equation and evaluate at  $y_l(k+1)$  yields

$$D(z^{-1})y_l(k+1) = C_lA_l \cdot x_f(k) + C_lB_l \cdot u_f(k)$$
 (15)

which can be further written as

$$y_l(k+1) = -y_l(k-\gamma+1) + C_l A_l \cdot x_f(k) + C_l B_l \cdot u_f(k).$$
(16)

An augmented state vector including the can be defined as

$$x_r(k) = \begin{bmatrix} x_f^T(k) & y_l^T(k) & \cdots & y_l^T(k-\gamma+1) \end{bmatrix}^T$$
(17)

and the augmented state-space system model can be written as:

$$x_r(k+1) = A_r \cdot x_r(k) + B_r \cdot u_f(k) + \overline{B_d} \cdot \varepsilon(k) \quad (18)$$

$$y_r(k) = C_r \cdot x_r(k) \tag{19}$$

where

$$A_r = \begin{bmatrix} A_l & O \\ \hat{C} & A_d \end{bmatrix}, \tag{20}$$

$$\hat{C} = \begin{bmatrix} C_l A_l \\ O \end{bmatrix}, \tag{21}$$

$$A_d = \begin{bmatrix} 0 & -I_{m \times m} \\ I_{(\gamma-1)n \times (\gamma-1)n} & 0 \end{bmatrix}$$
 (22)

where m is the number of dimensions of system output  $y_l(k)$ . Additionally, we have

$$B_r = \begin{bmatrix} B_l \\ C_l B_l \\ O \end{bmatrix}, \tag{23}$$

$$\overline{B_d} = \begin{bmatrix} B_d \\ O \end{bmatrix}, \tag{24}$$

$$C_r = [O_{n \times m} \quad I \quad O \quad \cdots \quad O]. \tag{25}$$

With the augmented system model that includes the disturbance model defined, an optimal controller that tracks the peeling angles can be designed. A linear quadratic regulator controller is then used. The controller is given by

$$u_f(k) = -K \cdot x_f(k) \tag{26}$$

The feedback gain K is obtained by using linear quadratic regulator (LQR). The actual torque control inputs can be computed as

$$u_{l}(k) = u_{f}(k) + u_{l}(k - \gamma)$$
 (27)

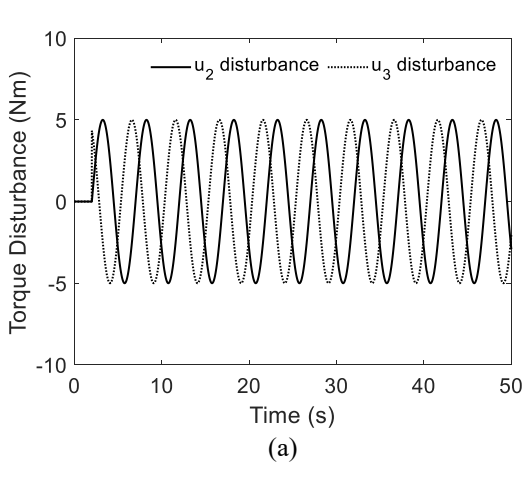
## 5. RESULTS

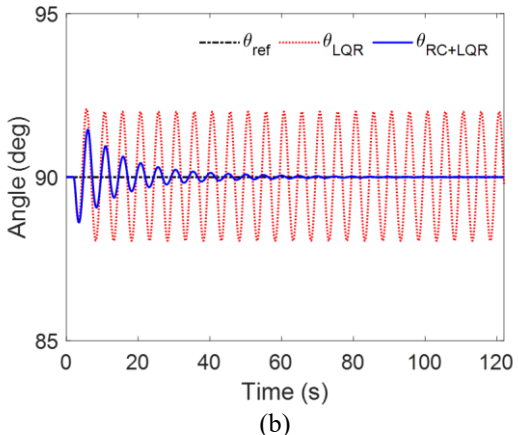
In this section, the repetitive controller designed in the previous section is validated with the nonlinear system model. In the simulation, two types of disturbances are considered: periodic torque disturbances on the rewinding rollers and periodic variation in the adhesion energy. Three simulation cases

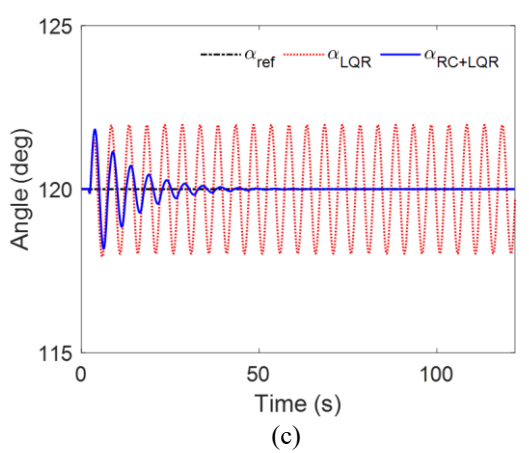
that represent typical operations of the R2R peeling process are presented here. The first case includes only the torque disturbances, the second case considers only the periodic adhesion energy variation, while the third case considers both the torque and adhesion energy disturbances simultaneously. The control objective is to maintain the peeling angles at  $\theta=90^\circ$  and  $\alpha=120^\circ$  at a line speed of 0.05m/s. A regular LQR controller that regulates the peeling angles and is designed based on the system model is compared with the LQR controller designed based on the repetitive control formulation.

In the first case, we introduce a sinusoidal torque disturbance with a frequency of 0.2 Hz, matching the rewinding roller frequency, and an amplitude of 5 Nm, as shown in Fig. 5(a). The torque disturbances are set to have a 90-degree phase difference.

The LQR controller and repetitive controller with perfect 5 seconds period information are simulated. The resulting peeling angles  $\theta$  and  $\alpha$  are shown in Fig. 5(b) and Fig. 5(c). It is shown that the angles are maintained around the desired level by both controllers. However, a periodic angle error exists throughout the simulation with the regular LQR controller. The repetitive controller, on the other hand, can reject the periodic disturbances and ends up with a perfect tracking of the peeling angles.

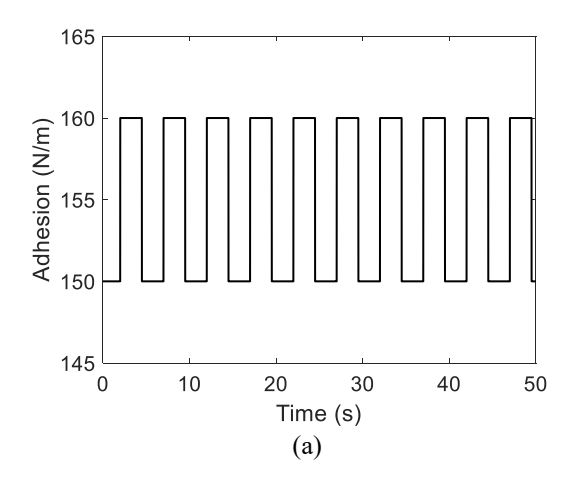






**FIGURE 5:** Torque disturbance simulation result (case 1) (a) torque disturbance, (b)  $\theta$  plot, and (c)  $\alpha$  plot

In the second case, we introduce the adhesion energy that is alternating between 150 N/m and 160 N/m with a period of 0.25 s. At a line speed of 0.05m/s, an adhesion disturbance with 5 seconds of period is introduced to the system, as shown in Fig. 6(a). The simulation results and zoom-in plots are shown in Fig. 6(b) and Fig. 6(c). It can be seen that the repetitive control method improves the performance and achieves better angle tracking over the entire time horizon compared to regular LQR only. However, because the adhesion energy is nonlinear, the linear model can only identify the adhesion fluctuations approximately. Therefore, the repetitive controller can only attenuate the effect of adhesion energy disturbance on the system dynamics.



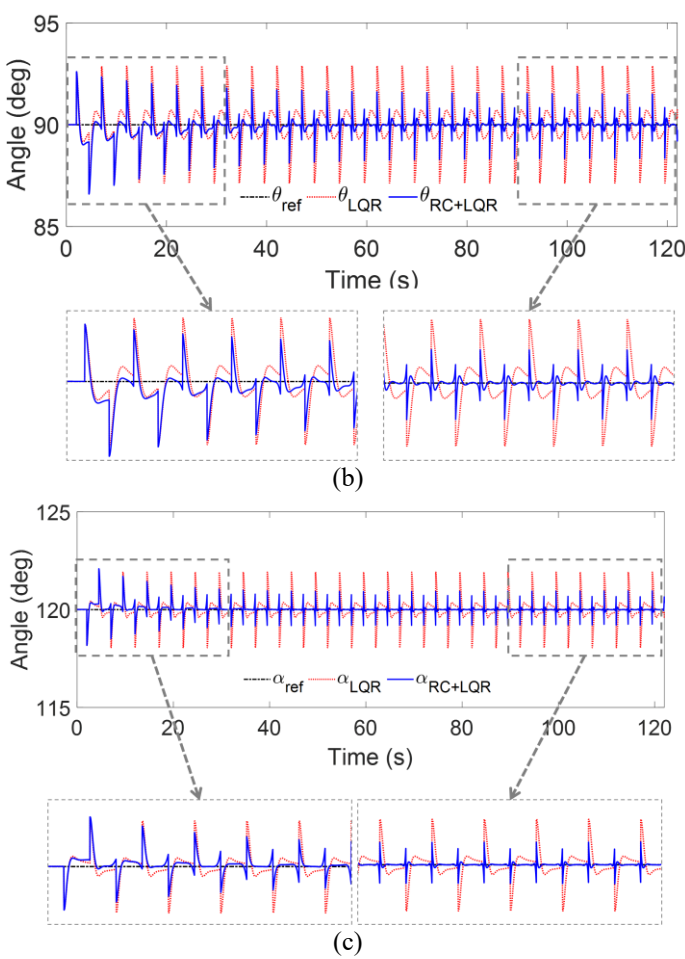


**FIGURE 6:** Adhesion energy disturbance simulation result (case 2) (a) adhesion energy change, (b)  $\theta$  plot, and (c)  $\alpha$  plot

In the third case, the two disturbances from the first and second case are introduced simultaneously. The two disturbance sources are of different frequencies. The frequency of the torque disturbances is set as 0.5 Hz (2 seconds of period). The adhesion energy change frequency is set to be the same as that in the second case, 0.2 Hz (5 seconds of period). Thus, the period of the disturbance in this case is 10 seconds, the least common multiple of the periods of the two disturbance sources. The simulation result is shown in Fig. 7. It can be seen that larger error is caused by the combined disturbances. The regular LQR controller struggles to maintain the peeling angles, while the repetitive control accounts for both disturbance sources and reduces the average angle error.

Table 1 compares the root-mean-square errors (RMSE) of the peeling angles associated with the repetitive controller against those of the regular LQR controller for each of the three cases. In each case the RMS angle error associated with the repetitive controller is significantly less than that associated with the regular LQR controller. Also, comparing case 1 to case 2, it seems that the repetitive control scheme can reject periodic disturbances in the torque better than periodic disturbances in the adhesion. Finally, when comparing how the two control schemes minimized the angle variation caused by changes in the adhesion energy alone (case 2), the RMS angle error associated with the

RC controller was less than one-third of that associated with the regular LQR controller.

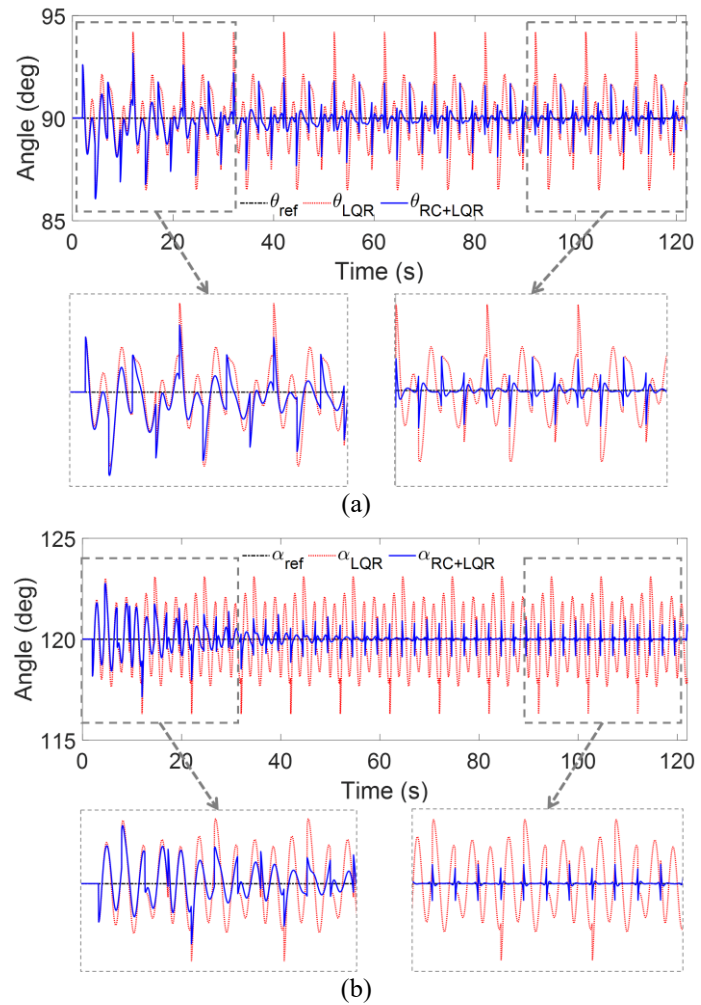


**FIGURE 7:** Torque disturbance and adhesion energy disturbance simulation result (case 3) (a)  $\theta$  plot, and (b)  $\alpha$  plot

TABLE 1. Simulation Case 3 Result Summary

Controller	Case 1 (Torque disturbance)		Case 2 (Adhesion variation)		Case 3 (Torque and adhesion variation)	
	θ RMSE (°)	α RMSE (°)	θ RMSE (°)	α RMSE (°)	θ RMSE (°)	α RMSE (°)
LQR	1.3947	1.3912	1.0908	0.5893	1.4504	1.5320
RC	0.0203	0.0036	0.3221	0.1511	0.3784	0.1736

## 6. CONCLUSION

A model-based repetitive control framework to maintain the desired R2R peeling angles is introduced in this study. The repetitive controller can reject the periodic disturbances that exist in the R2R system, such as torque and adhesion energy variations, with only knowledge of the disturbance's frequency. A system identification method is also used to obtain a linear system model for feedback control design. Simulation studies have shown the integrated repetitive control and system identification can provide better angle tracking performance than

feedback only. Future work includes implementing and validating the control strategy on a R2R dry transfer system.

#### **ACKNOWLEDGEMENTS**

This work is based upon work supported primarily by the National Science Foundation under Cooperative Agreement No. EEC-1160494 and CMMI-2041470. Any opinions, findings and conclusions or recommendations expressed in this material are those of the author(s) and do not necessarily reflect the views of the National Science Foundation.

#### **REFERENCES**

- [1] E. S. Polsen, D. Q. Mcnerny, B. Viswanath, S. W. Pattinson, and A. John Hart, "High-speed roll-to-roll manufacturing of graphene using a concentric tube CVD reactor," *Scientific Reports*, vol. 5, no. 1, p. 10257, 2015-09-01 2015, doi: 10.1038/srep10257.
- [2] Z.-Y. Juang *et al.*, "Graphene synthesis by chemical vapor deposition and transfer by a roll-to-roll process," *Carbon,* vol. 48, no. 11, pp. 3169-3174, 2010-09-01 2010, doi: 10.1016/j.carbon.2010.05.001.
- [3] S. Khan, L. Lorenzelli, and R. S. Dahiya, "Technologies for Printing Sensors and Electronics Over Large Flexible Substrates: A Review," *IEEE Sensors Journal*, vol. 15, no. 6, pp. 3164-3185, 2015-06-01 2015, doi: 10.1109/jsen.2014.2375203.
- [4] C. Linghu, S. Zhang, C. Wang, and J. Song, "Transfer printing techniques for flexible and stretchable inorganic electronics," *npj Flexible Electronics*, vol. 2, no. 1, 2018-12-01 2018, doi: 10.1038/s41528-018-0037-x.
- [5] X. Feng, M. A. Meitl, A. M. Bowen, Y. Huang, R. G. Nuzzo, and J. A. Rogers, "Competing Fracture in Kinetically Controlled Transfer Printing," *Langmuir*, vol. 23, no. 25, pp. 12555-12560, 2007-12-01 2007, doi: 10.1021/la701555n.
- [6] Z. Qin, Z. Xu, and M. J. Buehler, "Peeling Silicene From Model Silver Substrates in Molecular Dynamics Simulations," *Journal of Applied Mechanics*, vol. 82, no. 10, p. 101003, 2015-10-01 2015, doi: 10.1115/1.4030888.
- [7] Q. Zhao, N. Hong, D. Chen, and W. Li, "Controlling Peeling Front Geometry in a Roll-to-Roll Thin Film Transfer Process," in *International Manufacturing Science and Engineering Conference*, 2020, vol. 84256: American Society of Mechanical Engineers, p. V001T05A017.
- [8] S. Cho, N. Kim, K. Song, and J. Lee, "Adhesiveless Transfer Printing of Ultrathin Microscale Semiconductor Materials by Controlling the Bending Radius of an Elastomeric Stamp," *Langmuir*, vol. 32, no. 31, pp. 7951-7957, 2016-08-09 2016, doi: 10.1021/acs.langmuir.6b01880.
- [9] M. A. Meitl *et al.*, "Transfer printing by kinetic control of adhesion to an elastomeric stamp," *Nature Materials*,

- vol. 5, no. 1, pp. 33-38, 2006-01-01 2006, doi: 10.1038/nmat1532.
- [10] Q. Zhao, N. Hong, D. Chen, and W. Li, "A Dynamic System Model for Roll-to-Roll Dry Transfer of Two-Dimensional Materials and Printed Electronics," *Journal of Dynamic Systems, Measurement, and Control*, vol. 144, no. 7, p. 071004, 2022.
- [11] C. Martin, Q. Zhao, S. Bakshi, D. Chen, and W. Li, "PLDI-Based Convexification for Roll-to-Roll Dry Transfer Control," *IFAC-PapersOnLine*, vol. 54, no. 20, pp. 469-474, 2021.
- [12] C. Branca, P. R. Pagilla, and K. N. Reid, "Governing Equations for Web Tension and Web Velocity in the Presence of Nonideal Rollers," *Journal of Dynamic*

- Systems, Measurement, and Control, vol. 135, no. 1, p. 011018, 2013-01-01 2013, doi: 10.1115/1.4007974.
- [13] L. Wang, "A tutorial on predictive repetitive control," in 2016 Australian Control Conference (AuCC), 2016-11-01 2016: IEEE, doi: 10.1109/aucc.2016.7868013.
- [14] Q. Zhao, C. Martin, N. Hong, D. Chen, and W. Li, "A Real time Supervisory Control fo Strategy Roll to Roll Transfer of 2D Dry Materials and Printed Electronics," presented at the 2022 IEEE/ASME International Conference on Advanced Intelligent Mechatronics, 2022. Submitted.